Electronic Supplementary Information (ESI)

Locally boosted Li_2S nucleation on VO_2 by loading carbon quantum dots for soft-packaged lithium–sulfur pouch cells

Ruoxuan Yang,‡[a] Yunfeng Zhang,‡[a] Xifang Chen,[a*] Lixian Song,[a] Yue Hu,[b*] Yingze Song*[a]

[a] State Key Laboratory of Environment-Friendly Energy Materials, School of Mathematics and Physics, Southwest University of Science and Technology, Mianyang, Sichuan 621010, China.
[b] Key Laboratory of Carbon Materials of Zhejiang Province, College of Chemistry and Materials Engineering, Wenzhou University, 325000, China.

Corresponding authors: yzsong@swust.edu.cn (Y. Song); chenxifang@swust.edu.cn (X. Chen) and yuehu@wzu.edu.cn (Y. Hu)

Keywords: Lithium–sulfur pouch cell, sulfur evolution, carbon quantum dot, vanadium dioxide, local conductivity

1. Experimental Section

Synthesis of VO_2.

0.4 g NH_4VO_3 was dissolved in a mixture of 90 mL deionized water and 10 mL ethanol, and the pH value was controlled to around 2.0 by using 1.0 mol L^{-1} hydrochloric acid solution. The as-attained mixture was transferred to a Teflon-lined autoclave with a volume of 200 mL, and followed by holding at 180 °C for 24 h. After rinsing and freeze-drying, the VO_2 product was achieved.

Synthesis of CQDs.

28 mg 1,3 dihydroxynaphthalene was dissolved in 20 mL anhydrous ethanol. After full dissolving, 4 mL hydrochloric acid was added and sonicated for 5 min to disperse the mixture. The above mixed solution was added into a Teflon-lined autoclave, and then placed in a thermostat with 190 ℃ for 10 h and naturally cooled to room temperature. 35 mL anhydrous ethanol was added into the Teflon-lined autoclave and sonicated for 15 min to obtain the crude solution of CQDs. Centrifuge the solution at 11,000 rpm for 15 min to remove the large particles and insoluble by-products to obtain the supernatant, and then filter the supernatant through a 0.22 μm needle filter, and then put the filtered supernatant into a clean beaker and dry it at 100 ℃ to obtain the CQDs solids by removing excess acid. The above solid was fully dissolved with 15 mL anhydrous ethanol and then filtered through a 0.22 μm needle filter to obtain a clarified CQD solution. The purified CQDs were obtained by chromatographic separation of the obtained CQDs using a mixture of methanol and dichloromethane as the eluent.

Synthesis of VO_2/CQDs.

0.25 g VO_2 was added into 20 mL mixture of 0.5 g L^{-1} CQDs and ethanol. After mixing for 12 h and drying, the final VO_2/CQDs product was obtained.

Preparation of S/VO_2/CQDs cathodes.

VO_2/CQDs, carbon black and sulfur were mixed at the mass ratio of 1:1:6, grinding uniformly. Then the mixture was heated at 155 ℃ for 12 h with the protection of Ar. After that, S/VO_2/CQDs, carbon black and LA133 were mixed at a mass ratio of 8:1:1. The S/VO_2/CQDs cathode was prepared by uniformly covering the slurry on aluminum foil and subsequently vacuum drying at 60 ℃ for 12 h.

Preparation of pouch cells.

The prepared cathode was cut at a size of 3×3 cm^2. In addition, 3.5×4 cm^2 copper foil was used as the collector, and the size of PP separator was 4.5×5 cm^2. The electrolyte/sulfur ratios are 7 μL mg^{-1} for single-layer pouch cells and 5 μL mg^{-1} for multi-layer pouch cells, respectively. The battery assembly process was carried out in an argon-filled glove box.

Material characterizations.

The morphology was examined using a MAIA3 model 2016 field emission scanning electron microscope from Tescan, Czech republic. Detailed structural and elementals were observed by Tecnai G2 F20 S-Twin transmission electron microscope with an accelerating voltage of 200 kV. X-ray diffraction patterns were recorded using FEI, tecnai F20-ray diffractometer. The infrared spectra were recorded by using TENSOR II infrared spectrometer. Thermo SCIENTIFIC K-Alpha X-ray photoelectron spectroscopy was performed to detect the surface chemical compositions of samples. The ultraviolet−visible absorption spectra were recorded using a TU-1901 dual beam ultraviolet−visible spectrometer. The sheet resistances of VO_2/CODs and VO_2 are tested by ROOKO FT-300I-300kg powder resistivity test system. Typically, 20 mg catalyst sample was dispersed into 50 mL isopropanol homogeneously. The as-obtained mixture was subsequently vacuum filtered on the polytetrafluoroethylene (PTFE) membrane, followed by drying for 24 h at room temperature.

Adsorption tests.

To obtain Li_2S_6 solution (5 mmol L^{-1}), the lithium sulfide and sublimed sulfur at a molar ratio of 1:5 was dissolved in 1,2-dime-thoxyethane solvent. With the same mass of 20 mg, VO_2/CQDs and VO_2 electrocatalysts were added into two bottles with 2 mL Li_2S_6 solution, respectively. The devices were placed in an argon-filled glove box.

Li_2S nucleation/ dissociation tests.

Li_2S_8 solution with a concentration of 0.2 mol L^{-1} was gained by the reaction of sulfur and Li_2S at a molar ratio of 1:7 in tetraglyme solvent. 0.005 g VO_2/CQDs or VO_2 was loading on a carbon paper with a diameter of 13 mm. All the nucleation cells were assembled by using lithium foil as the anode, the as-prepared Li_2S_8 solution (20 μL) as the catholyte, and 20 μL LiTFSI solution as the anolyte. The cells were galvanostatically discharged under 0.112 mA until the potential was 2.06 V and subsequently kept potentiostatically at 2.05 V till the current reaches 10^{-5} A. Similarly, the dissociation tests were first performed galvanostatically at a current of 0.112 mA until the potential

was below 1.7 V. Subsequently, the cells were potentiostatically charged at 2.35 V to 10^{-5} A. The nucleation capacity of Li_2S was calculated according to Faraday's Law.

Electrochemical tests.

The Neware CT4008 battery tester was used to evaluate the electrochemical performance of pouch cells, including the charge and discharge curves, rate capacities and cycle stability. Cyclic voltammetry curves and electrochemical impedance spectroscopy were recorded on a Metrohm Autolab G204 electrochemical workstation.

2. Figures

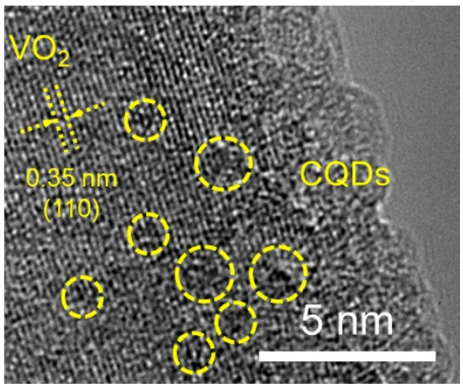

Fig.S1 HRTEM image of VO_2/CQDs

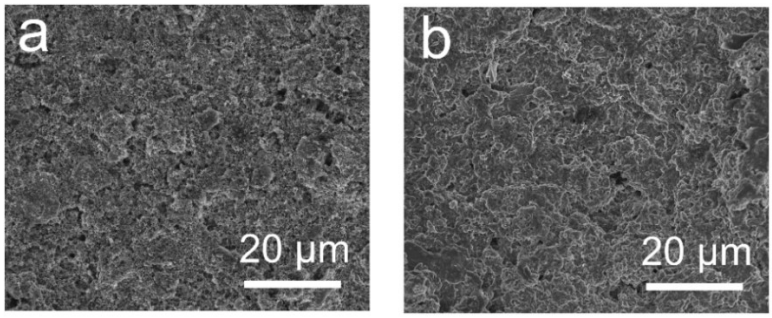

Fig. S2 SEM images of S/VO_2/CQDs (a) before and (b) after cycling.

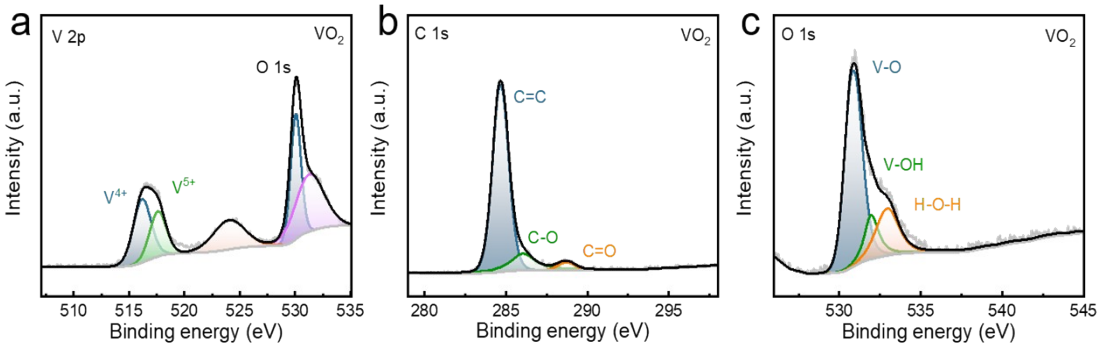

Fig. S3 XPS high-resolution spectra of VO_2: (f) V 2p, (g) C 1s and (h) O 1s.

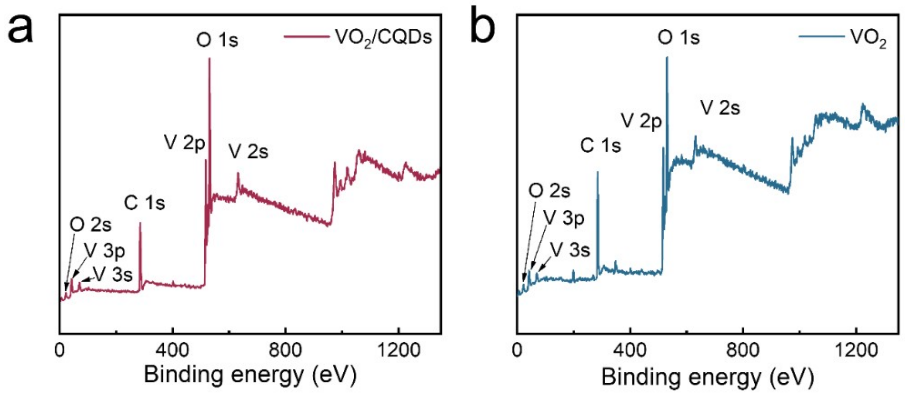

Fig. S4 XPS survey sp·trum of (a)VO_2/CQDs and (b) VO_2.

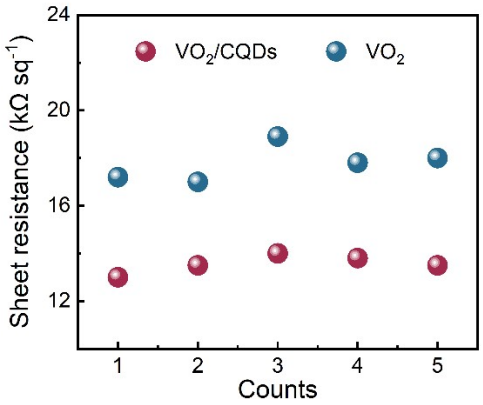

Fig. S5 Sheet resistances of VO_2/CQDs and VO_2.

VO_2/CQDs shows a higher sheet resistance average value of 13.5 kΩ sq^{-1} compared with the bare VO_2 (17.7 kΩ sq^{-1}) due to the introduction of CQDs (Fig. S5).

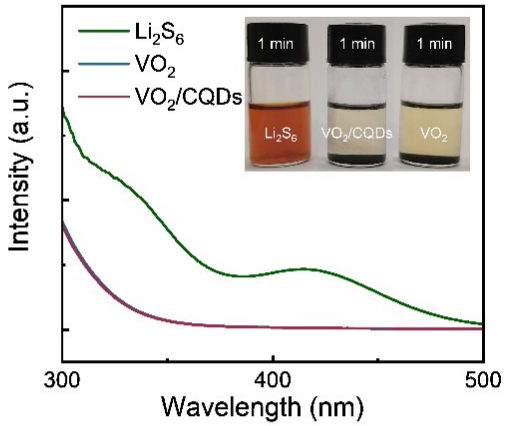

Fig. S6 UV–vis absorption spectra of a Li_2S_6 solution after adsorptions.

In Fig. S6, the both samples can completely fade Li_2S_6 solution within 1 min, and the Li_2S_6 absorption signals in the visible light range vanish according to the UV–vis absorption spectra. These results substantiate the high LiPS adsorption efficiencies of the two samples and that the addition of CQDs doesn't change the unique LiPS adsorption model.

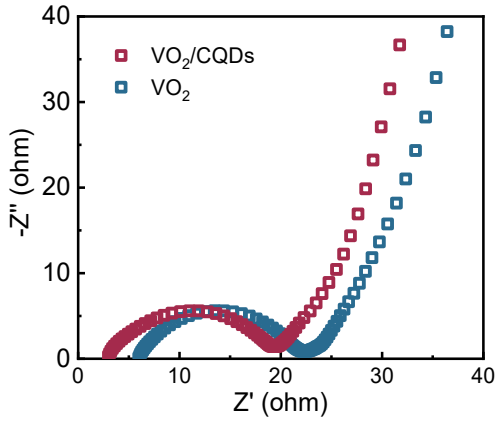

Fig. S7 EIS of S/VO_2/CQDs and S/VO_2.

Fig. S7 shows the electrochemical impedance spectroscopy (EIS) profiles of the batteries by using the two samples as the catalysts. The charge transfer resistances (R_{ct}) of VO_2/CQDs and VO_2-based batteries are 16.3 and 16.5 Ω, respectively, indicating that the CQDs don't elevate the electron conductivity of the whole sulfur cathode but only tune the local electron conductivity of VO_2 surface.

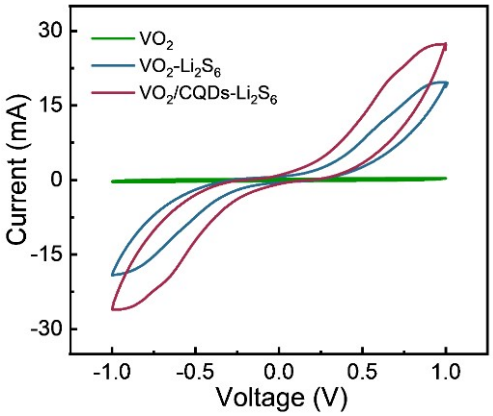

Fig. S8 CV curves of the symmetric cells at 50 mV s^{-1} between –1 and 1 V.

The CV curve of symmetrical battery at 50 mv s^{-1} show that VO_2/CQDs has a higher redox current than the bare VO_2, demonstrating its elevated catalytic activity (Fig. S8).

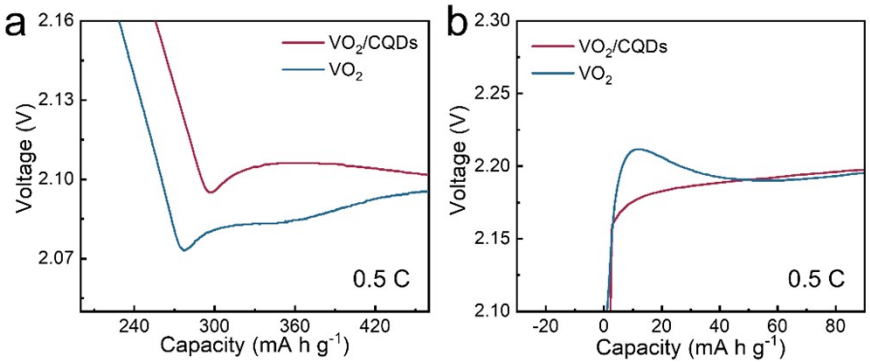

Fig. S9 Partial discharge and charge curves of different cathodes.

Based on the partial curves of discharge and charge profiles, the VO_2/CQDs cathode endows the lower overpotentials for both the sulfur reduction and oxidation procedures owing to the introduction of CQDs (Fig. S9). Li^+ diffusion rate usually makes large contribution to the kinetically promoted sulfur reactions.

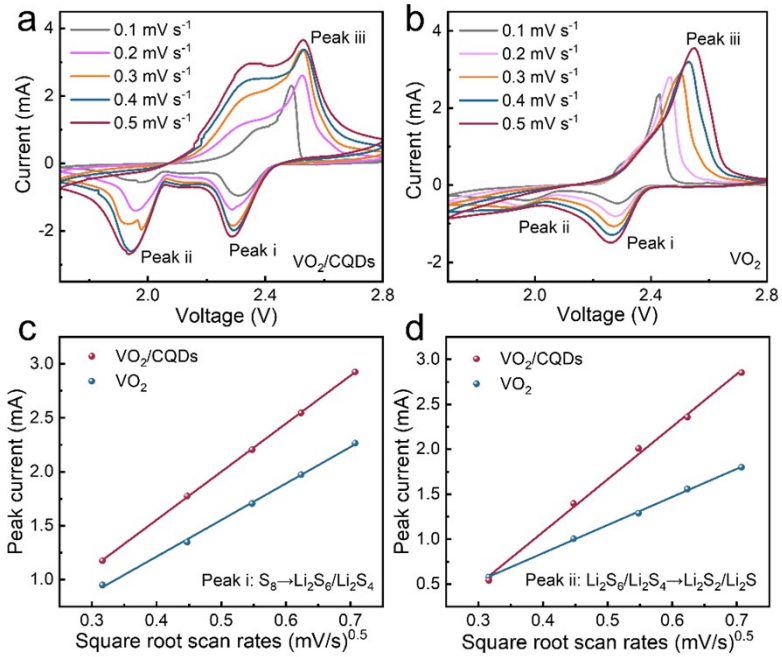

Fig. S10 CV curves of S/VO_2/CQDs (a) and S/VO_2 (b) at different sweep rates, and (c, d) Li^+ diffusion properties originating from the CV curves in (a) and (b).

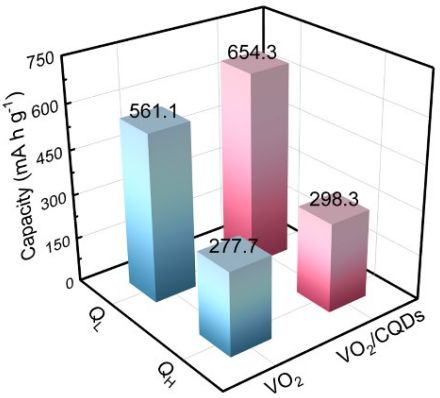

Fig. S11 The statistic capacities which are contribued by the two plateaus of S/VO_2/CQDs and S/VO_2.

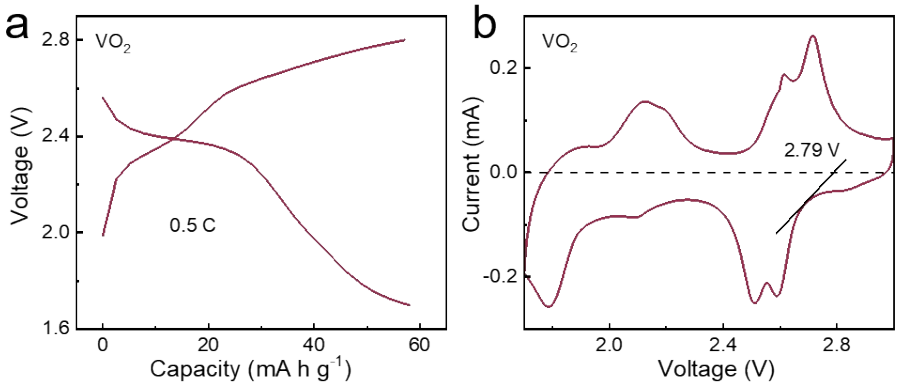

Fig. S12 GCD (a) and CV (b) curves of VO_2.

The galvanostatic charge/discharge (GCD) and CV plots of pure VO_2-based cathodes are shown in Fig S12. According to the GCD curve of bare VO_2 cathode in Fig. S12a, VO_2 with a low content of 10 wt% shows a relatively low contribution to the entire battery capacity. The CV profile of bare VO_2-based cathode in Fig. S12b shows the redox potential of 2.79 V, displaying its redox potential in the sulfur reaction window.

Table S1 Comparison of battery performances between this work and reported studies.

Catalyst	Rate (C)	Cycle number	Discharge capacity (mA h g^{-1})	Capacity retention (%)	Ref.
VO_2/CQDs	0.5	100	952.6	88.8	This work
VO_2/CQDs	2	200	724.5	64.3	This work
S/V-N-C	0.2	100	882.1	-	1
MoB/S	0.05	55	947	-	2
PHPCC@S	0.2	30	733	72.0	3
IHPC-2/S (93)	0.1	40	1162	83.8	4
S/Ni-N-C 850	0.1	100	1265.4	81.3	5
PhSeH	0.02	20	1398	83.3	6
V_2O_3/V_8C_7@C@G	0.2	150	716.8	-	7
ICFs/nS/rGO	0.1	51	1156.7	76.6	8

The as-designed Li–S batteries with VO_2/CQDs as the catalyst show surpassing cycling performance compared the reported pouch cells (Table S1).

References

1. S. Yu, Y. Sun, L. Song, X. Cao, L. Chen, X. An, X. Liu, W. Cai, T. Yao, Y. Song and W. Zhang, *Nano Energy*, 2021, **89**, 106414.

2. J. He, A. Bhargav and A. Manthiram, *Adv. Mater.*, 2020, **32**, 2004741.

3. J. Zhang, C. You, J. Wang, H. Xu, C. Zhu, S. Guo, W. Zhang, R. Yang and Y. Xu, *Chem. Eng. J.*, 2019, **368**, 340.

4. L. Wang, S. Liu, J. Hu, X. Zhang, X. Li, G. Zhang, Y. Li, C. Zheng, X. Hong and H. Duan, *Nano Res.*, 2021, **14**, 1355.
5. X. Cao, M. Wang, Y. Li, L. Chen, L. Song, W. Cai, W. Zhang and Y. Song, *Adv. Sci.*, 2022, **9**, 2204027.
6. J. Sun, K. Zhang, Y. Fu and W. Guo, *Nano Res.*, 2023, **16**, 3814.
7. L. Zhang, Y. Liu, Z. Zhao, P. Jiang, T. Zhang, M. Li, S. Pan, T. Tang, T. Wu, P. Liu, Y. Hou and H. Lu, *ACS Nano*, 2020, **14**, 8495.
8. F. Wu, Y. Ye, J. Huang, T. Zhao, J. Qian, Y. Zhao, L. Li, L. Wei, R. Luo, Y. Huang, Y. Xing and R. Chen, *ACS Nano*, 2017, **11**, 4694.